Effect of the non-dipole field on the seasonal variation of the geomagnetic Sq(Y)

Lin Tian[1, 2], Aimin Du[1, 2, *], Sheng Huang[1], Hao Luo[1, 2, *], Wenyao Xu[1, 2], Yasong Ge[1, 2]

[1]Key Laboratory of Earth and Planetary Physics, Institute of Geology and Geophysics, Chinese Academy of Sciences, Beijing 100029, China;

[2]College of Earth Science, University of Chinese Academy of Sciences, Beijing, China

Corresponding author: Hao Luo (luohao06@gmail.com); Aimin Du (amdu@mail.igcas.ac.cn)

Key points:

1. The Sq(Y) at 25 mid-low observatories were statistically investigated by decomposing into different timescales.
2. Annual mean, annual variations, and semiannual variations were analyzed with respect to the geomagnetic components.
3. The non-dipole filed has strong effects on Sq(Y) with different timescales.

Abstract. Different timescales of the daily amplitude of the geomagnetic Y component during quiet period (Sq(Y)) over several solar cycles at 25 mid-low latitudes observatories were analyzed. The annual mean (Sq_0), annual (Sq_1) and semiannual (Sq_2) components were separated from Sq(Y) by means of Fourier

analysis method. No obvious distinction is found for the morphology of the spatial distribution of these Sq(Y) components during solar quiet and active periods, except that they are more intense in high solar activity. Sq_1(Y) exhibits a remarkable longitudinal inequality, which is much stronger around Eurasia and Australia anomaly zones and weaker around South Atlantic Ocean anomaly (SAO) zones. The positive correlation between Sq_0(Y) and geomagnetic vertical component *Z* suggests that the convection electric fields in the dynamo region play a key role in controlling annual mean (Sq_0). On the other hand, the Sq_1(Y) exhibits a positive correlation with geomagnetic horizontal component *H*, implying the inter-hemispheric field-aligned currents (IHFACs) may contribute to difference of the annual variation amplitude at different observatories. The Sq_2(Y) is most prominent in the SAO region. It is possible the stronger ionospheric conductivity in the dynamo region contribute to the remarkable semiannual variation in SAO region.

1. Introduction

It is well known that the solar quiet daily geomagnetic variation (Sq) at mid-low latitudes primarily originated from the dayside ionospheric E-region dynamo [Matsushita, 1967; Forbes and Lindzen, 1976; Richmond, 1979; Yamazaki et al., 2017]. According to the classical dynamo theory, the distribution of the Earth's main field in space, the tidal wind, and the ionospheric conductivity control the behavior of the Sq type variation [Campbell, 1982]. In particular, the geomagnetic field not only modulates the conductivity through its dependence on the electron and ion gyrofrequencies, but also controls the dynamo electric field [Stening, 1971; Takeda,

1996; Le Sager and Huang, 2002]. As a consequence of these factors, the Sq electric current systems show a remarkable dependence on season, solar activity, longitudinal zone and hemisphere [*Matsushita and Maeda*, 1965; Campbell, 1982; Takeda, 1999, 2002a; Pedatella et al., 2011; Yamazaki et al., 2011].

The seasonal variation of Sq is identified by the ground-based [Currie, 1966; Banks and Nullard, 1966; Wagner, 1969; Bhargava, 1972; Campbell, 1982; Takeda, 1999; 2002a; Yamazaki et al., 2009] and satellite magnetometers [e.g. sPedatella et al., 2011]. The Sq intensity shows a conspicuous annual variation at each hemisphere [e.g., Matsushita and Maeda, 1965; Takeda, 2002a]. It enhances during the local summer and decreases during the local winter. This is consistent with the annual change of the insolation and E-region ionization level [Yamazaki et al., 2009]. A distinct semiannual variation of the Sq intensity with maxima near the equinoxes and minima near the solstices is also found [*Campbell and Matsushita*, 1982; Hibberd, 1985; Stening, 1995; Takeda, 1999, 2002a; Pedatella et al., 2011], however its incidence varies with hemisphere, longitude and local time [Stening, 1995]. In contrast, the seasonal variation of the foci of the Sq current system is more complicated. Typically, the foci are located between 30^{o} and 35^{o} dip latitudes [Matsushita and Maeda 1965]. Previous studies suggested that the northern foci moved poleward notably during September-November and the southern foci moved equatorward during January-February [Hasegawa, 1965; Tarpley, 1973; Stening et al, 2007]. Such foci shift in position is generally accompanied with the variation of the electrojet amplitude at the equator and could be associated with the variations in the

67 tidal winds in the ionosphere [Campbell, 1982; Stening and Reztsova, 2005; Stening
68 et al., 2007].

69 The influence of solar activity on Sq has also been studied for decades [e.g.,
70 Chapman and Bartels, 1940; Chapman et al., 1971; Rastogi and Iyer, 1976; Campbell
71 and Matsushita, 1982; Briggs, 1984; Takeda et al., 1986; Takeda, 2002b, 2013a, b].
72 When the sunspot number (SSN) increases, the Sq amplitude enhances along with the
73 increasing height integrated Pedersen and Hall conductivities in the ionosphere
74 [Rastogi and Iyer, 1976; Briggs, 1984; Takeda, 2002b, 2013a]. The Sq current in the
75 solar active year is about 1.6 to 3.0 times as large as that in the solar quiet year with
76 the larger ratio occurring in mid-November [Campbell and Matsushita, 1982]. The
77 seasonal change of the Sq varies with solar activity level as well [Chapman et al.,
78 1971; Takeda, 2013a]. Campbell and Matsushita [1982] compared the Sq behavior in
79 North American zones during solar active and quiet periods. They found that the Sq
80 amplitude showed a dominant annual variation in the quiet year and a dominant
81 semiannual variation in the active year. The semiannual variation was also
82 conspicuous for sum of the northern and southern current intensities with maximum at
83 April and at October or November in solar maximum years [Takeda, 1999, 2002a].
84 Since the relative amplitude of semiannual variation in Sq is much higher than that for
85 the ionospheric conductivity, it is impossible to explain the semiannual variation of Sq
86 intensity without taking into account other processes independent on the conductivity
87 [Wagner et al., 1980; Yamazaki et al., 2009].

88 It is demonstrated that the Sq current whorls with the focus at the mid latitude is

89 rather stable, regardless of the solar-terrestrial conditions [Campbell and Matsushita,
90 1982; Yamazaki et al, 2011]. Thus, the geomagnetic Y components at the mid-low
91 latitude are reflected by equatorward current in the morning side and poleward current
92 in the afternoon side. Takeda [2013a] analyzed the daily variation of the geomagnetic
93 Y component (Sq(Y)) in several long-term operated observatories and found an
94 obvious seasonal variation of Sq(Y), strongly dependent on the solar activity.
95 Furthermore, the strength of the seasonal variation of Sq(Y) varies with its geographic
96 location [Takeda, 2013a; 2013b]. The longitudinal inequalities in the Sq current
97 system and its seasonal variation were also identified by the CHAMP satellite
98 magnetic field observations [Pedatella et al., 2011]. By means of spherical harmonics
99 analysis (SHA), Matsushita and Maeda [1965] revealed the features of the Sq current
100 system in Asia-Australia, Europe-Africa and America Sectors and suggested the
101 longitudinal variability was caused by the differences of the relative position of the
102 geomagnetic and the geographic equators. Modeling results also clearly showed a
103 strong dependence of the Sq current system on the longitudinal variation of the
104 geomagnetic field [Stening, 1971; Le Sager and Huang, 2002].

105 Although there is no doubt that the geomagnetic field plays an important part in
106 generating longitudinal variations in the Sq current system [Stening, 1971; Pedatella
107 et al., 2011], the effects of the magnetic fields, especially the non-dipole field parts
108 on the longitudinal and variabilities of Sq with different timescales remains an open
109 question. A detailed investigation on seasonal variations of Sq in non-dipole
110 geomagnetic anomaly, which strongly distorts the morphology of the geomagnetic

dipole field, is very helpful for understanding the effect of the geomagnetic field on Sq. In this study, we examine the spatial distribution of seasonal variations of Sq(Y) in mid-low latitudes, and discuss its correlation with the geomagnetic field.

2. Data analysis

The one-hour geomagnetic data analyzed in this work are obtained at 25 mid-low latitude stations from World Data Center for Geomagnetism, Edinburgh (http://www.wdc.bgs.ac.uk/catalog/master.html). Table 1 lists the names and the geographic and geomagnetic coordinates of these stations and **Figure 1** shows the geographic distribution of them. Although the longitudinal distribution is quite inhomogeneous, the stations cover most longitudinal zones in both hemispheres. All stations have operated for at least one solar cycle and 80% of them provide available data for more than 20 years (listed in Table 1).

To avoid the effect of the magnetic disturbance, the geomagnetic data were selected in days (in local time) when the maximum of the geomagnetic disturbance index Kp is no more than 2+. In consideration of the day-to-day variability in the Sq geomagnetic field [Stening and Reztsova, 2005; Chen, et al, 2007], one-hour values of the geomagnetic data at each local time were averaged over a month to produce the monthly mean data.

In general, the geomagnetic horizontal components H have very different behavior for different longitudinal sectors in equinoctial months, with a positive peak around noon in the Asian and African sectors, but with a negative peak around noon in the American sector [Matsushita and Maeda, 1965; Campbell, 1989; Le Sager and

133 Huang, 2002]. In contrast, for *Y* components, it is relatively regular without large
134 longitudinal phase changes. Thus, the monthly mean one-hour values of the
135 geomagnetic *Y* component were chosen to investigate their seasonal variations in the
136 present study. The daily variation of *Y* (Sq(Y)) is obtained as the difference between
137 the maximum value in the morning (afternoon) side and the minimum value in the
138 afternoon (morning) side in the northern (southern) hemisphere in the daytime
139 [Takeda, 2002b, 2003a, b; Takeda et al., 2003]. The averaged horizontal and vertical
140 components of the geomagnetic data in nocturnal intervals (0-1 LT) were calculated
141 as a proxy of the geomagnetic main field at each station.

142 In consideration of intensive influence of the solar activity on Sq field, we made a
143 comparison of Sq(Y) in the high and low solar activity state. Three maximum and
144 minimum sunspot number years in each solar cycle were classified as higher and
145 lower solar activity years. As shown in **Figure 2**, the high solar activity years show
146 large variations in sunspot number (SSN) and Sq(Y) from one solar maximum to
147 another (red dots). Since Sq(Y) has a pronounced linear dependence on monthly mean
148 SSN, we normalized Sq(Y) to SSN=150 and SSN=20 for high and low solar activity
149 years, relying on the linear relationship between Sq(Y) and SSN.

150 **2.1 Spatial distribution of seasonal variations of Sq(Y)**

151 **Figure 3** shows the variations of Sq(Y) at KNY(130.9^{o} E, 31.4^{o} N) and CTA
152 (146.3^{o} E, 20.1^{o} S) in Asia-Australia sector (**Figures 3a, 3b**), at TAM (5.5^{o} E, 22.8^{o} N)
153 and TSU (17.6^{o} E, 19.2^{o} S) in Europe-Africa sector (**Figures 3c, 3d**), and at SJG (66.2
154 ^{o} W, 18.1^{o} N) and PIL (63.9^{o} W, 31.7^{o} S) in America sector (**Figures 3e, 3f**) in the

155 northern hemisphere (left column) and the southern hemisphere (right column),
156 respectively. It is noted that a similar semiannual or annual variation in Sq(Y) at one
157 station is shown in **Figure 3** for both solar maximum and minimum years. The
158 amplitude of Sq(Y) in the higher solar maximum years (red triangles) is about 40%
159 more intensive than that in solar minimum years (blue diamonds) in the three sectors.
160 For northern hemispheric stations, the Sq(Y) enhances in March and declines in
161 October, and no apparent amplitude dip appears in June solstices. These observational
162 characteristics indicate the coupling of an annual variation with a peak of June and a
163 semiannual variation with two peaks of March and September. The annual variations
164 are larger than the semiannual variations in the northern hemisphere. The amplitudes
165 of annual variations are strongest in KNY and weakest in SJG. The annual
166 characteristics of Sq(Y) are in agreement with the observations by Rastogi et al. [1994]
167 in Indian region and by Yamazaki et al. [2009] in 210^{o} magnetic meridian (MM)
168 chain.
169 By contrast, the semiannual variations are prominent for stations in the southern
170 hemisphere. The peaks of the seasonal variation appear in February and October in
171 CTA station. The semiannual variations significantly enhance and play an important
172 role in the African and South American zones (**Figures 3d, 3f**). However, it is clearly
173 noted that the annual variation is also strong at CTA in the Australian zone (**Figure**
174 **3b**). The ground-based magnetometers and CHAMP satellite magnetometers have
175 revealed that the seasonal variation in the Europe-Africa longitudinal sector of the
176 southern hemisphere exhibits a primarily semiannual oscillation with maxima near

177 equinoxes [Pedatella et al., 2011]. It also can explain the controversy of observations
178 by Campbell and Matsushita [1982] and Stening [1995]. Campbell and Matsushita
179 [1982] using data from North America stations noted that the semiannual Sq variation
180 is distinct only during solar maximum period. However, Stening [1995] using data
181 from global stations reported the semiannual Sq variation even during solar minimum
182 period. One of the reasons causing the diversity of seasonal variation during
183 maximum and minimum period is the dependence of semiannual variation of the
184 strength of Sq(Y) on the geographic location.

185 We use Fourier harmonic analysis method [referring to Campbell, 1989] to
186 separate the annual and semiannual variations from Sq(Y) for 25 stations. 12 monthly
187 mean values of Sq(Y) averaged over all the low (or high) solar activity years were
188 used to compute the Fourier harmonic components. The first three Fourier harmonics
189 roughly represent the variations with periods of ~0, 1, and 0.5 years, respectively. We
190 sign them as the stationary component, $Sq_0(Y)$, annual component, $Sq_1(Y)$, and
191 semiannual component, $Sq_2(Y)$, respectively. The synthesis of the first three Fourier
192 harmonic is in good agreement with the observed data (not shown in this paper).

193 **Figure 4** shows the longitudinal distribution of $Sq_1(Y)$ and $Sq_2(Y)$ in the northern
194 (left panels) and southern (right panels) hemispheres. In the northern hemisphere, the
195 annual component $Sq_1(Y)$ is quite strong in the Asian sector (red line) and very weak
196 in the North American sector (blue line). In contrast, the semiannual component
197 $Sq_2(Y)$ for most northern stations are not so strong as Sq1(Y) both in solar quiet and
198 active periods. The approximately equal values of Sq1(Y) and Sq2(Y) in North

American stations indicate the existence of the semiannual variation previously reported [*Campbell and Matsushita*, 1982].

In the southern hemisphere, the annual variation of $Sq_1(Y)$ is prominent in the Australian sector (red line), while much weaker in the African sector (blue line). $Sq_2(Y)$ is strong in the Australian and African stations and quiet weak in the Pacific stations. Notably, $Sq_2(Y)$ around the South Atlantic anomaly zone, such as the African station TSU and the South American station PIL, is extremely intense compared to $Sq_1(Y)$, indicating that the semiannual variation dominate in this zone.

Figure 5 shows the latitudinal distribution of $Sq_1(Y)$ and $Sq_2(Y)$ in the Asia-Australia sector (left panels) and the Europe-Africa sector (right panels). In the Asia-Australia sector, the annual component $Sq_1(Y)$ shows no obvious difference between the two hemispheres, and is slightly weaker in the equatorward station. $Sq_2(Y)$ in the northern hemispheric station is quiet weak in the solar quiet period, and becomes intense in the solar active period, as well as the Australian station PMG. In the Europe-Africa sector, asymmetric distribution of $Sq_1(Y)$ and $Sq_2(Y)$ between the two hemispheres is clearly demonstrated. $Sq_1(Y)$ in the southern hemisphere is much weaker than that in the northern hemisphere. On the contrary, $Sq_2(Y)$ in the southern hemispheric station are fairly strong in both the solar quiet and active periods, while $Sq_2(Y)$ in the northern hemispheric stations TAM and MBO are still quite weak.

2.2 Correlation of Sq(Y) with the geographic latitude and components of the geomagnetic field

Figure 6 depicts the correlation of $Sq_0(Y)$ with the geographic latitude, φ, and

221 horizontal component, *H*, and vertical component, *Z*, of the geomagnetic field for
222 northern (left column) and southern (right column) hemispheres. The stationary
223 component $Sq_0(Y)$ enhances with increasing φ and *Z* for both high and low solar
224 activity years. It is surprising that $Sq_0(Y)$ increases with decreasing of *H*. The slope of
225 the linear fit during high solar activity years is generally larger than during low solar
226 activity years.

227 The annual component $Sq_1(Y)$ exhibits a significantly different relationship with
228 the geographic latitude and the geomagnetic components (shown in **Figure 7**). $Sq_1(Y)$
229 increases with increasing φ in the northern hemisphere, while reverses in the southern
230 hemisphere. Instead, a better correlation between $Sq_1(Y)$ and *H* was found in both
231 hemispheres (**Figures 7c and 7d**). Notably, the slope for the northern hemisphere was
232 steeper than that for the southern hemisphere both in low and high solar activity. No
233 obvious correlation between $Sq_1(Y)$ and the vertical component *Z* is found in both
234 hemispheres.

235 The correlation of the semiannual component $Sq_2(Y)$ with the geographic latitude
236 and the geomagnetic components is quite different in northern and southern
237 hemispheres (shown in **Figure 8**). In the northern hemisphere, $Sq_2(Y)$ is rather small
238 in solar quiet condition, and shows no significant correlations with the geographic
239 latitude and *H*. Only a slight positive correlation between $Sq_2(Y)$ and *Z* is detected. In
240 the high solar activity, $Sq_2(Y)$ is positively relevant to φ and *H*. In the southern
241 hemisphere, $Sq_2(Y)$ becomes weaker in the lower latitude (**Figure 8b**) and intensifies
242 as the geomagnetic component *H* decreases (**Figure 8d**), in spite of the

243 solar-terrestrial condition. Similar to $Sq_1(Y)$, no distinct correlation with *Z* was found
244 for $Sq_2(Y)$.

245 The correlation coefficients between Sq(Y) and the geographic latitude and
246 components of the geomagnetic field are listed in Table 2. It suggests that the
247 stationary component $Sq_0(Y)$ is significantly correlated with the geomagnetic vertical
248 component *Z* and the annual component $Sq_1(Y)$ is significantly correlated with the
249 geomagnetic horizontal component *H*. $Sq_2(Y)$ in the northern hemisphere shows no
250 significant correlation with the geographic latitude and the geomagnetic field. In
251 contrast, $Sq_2(Y)$ in the southern hemisphere correlated well with the geographic
252 latitude and *H*. Additionally, $Sq_0(Y)$ in the northern hemisphere also shows a
253 prominent relationship with the geographic latitude.

254 **3. Discussions and Conclusions**

255 It is well known that the geomagnetic non-dipole field zones are five large-scale
256 anomalies (Xu and Bai, 2009), which are listed according to their maximum
257 intensities as follows: the South Atlantic Ocean anomaly (SAO), Africa anomaly
258 (AFR), Eurasia anomaly (ERA), Australia anomaly (AST), and North America
259 anomaly (NAM). In particular, the two strongest negative anomalies (defined in total
260 intensity) SAO and AFR dramatically distort the morphology of the geomagnetic field
261 in the African sector as shown in **Figure 1**. In these African stations, Sq(Y) shows
262 distinctive seasonal variations as well, where the semiannual variation is dominant
263 both in the solar active and quiet periods.

264 Many studies have demonstrated that the geomagnetic field plays a key role in

generating longitudinal variations in the Sq current system [Stening, 1977; Pedatella et al., 2011]. Pedatella et al. [2011] took into account the influence of non-migrating tides to account for the longitudinal variability. In our study, we compared the correlation between the seasonal components of Sq(Y) and the geomagnetic field components. It provides another way to investigate the cause of the longitudinal variability of Sq.

According to the classic dynamo theory, the geomagnetic main field controls the convection electric field of the Sq dynamo [Stening, 1971]. Weakening of the magnetic field decreases the electrostatic potential difference and increases the height-integrated ionospheric Pederson and Hall conductivity [Takeda, 1996]. Hence, the positive correlation between Sq_0(Y) and the geomagnetic vertical component *Z* suggests that the ascending *Z* increases Sq_0(Y) monotonously by means of enhancing the electrostatic potential. The negative correlation between Sq_0(Y) and the geomagnetic horizontal component *H* implies that *H* affects Sq_0(Y) by virtue of altering the ionospheric conductivity. In fact, the correlation coefficients between Sq_0(Y) and *Z* are 0.83/0.81 in the northern/southern hemisphere during solar maximum, whereas those between Sq_0(Y) and *H* are 0.49/0.36, indicating that Sq_0(Y) significantly correlates with *Z* and insignificantly correlates with *H*. It suggests that Sq_0(Y) could be primarily influenced by the plasma drift electric field and controlled by geomagnetic vertical component *Z*. On the other hand, although the South American station PIL located at the similar geomagnetic latitude (21.4ºS) with the African station TAN (23.7ºS) and the Australian station KDU (22.1ºS), Sq_0(Y) in PIL

287 during solar maximum (52.2 nT) are much weaker than that in TAN (63.2 nT) and
288 KDU (63.3 nT). It is worth noting that the Sq(Y) in South American sector stations is
289 strongly affected by South Atlantic Ocean anomaly. The geomagnetic vertical
290 component *Z* in PIL (~11900 nT) is much weaker than that in TAN (~27500 nT) and
291 KDU (~30100 nT). In consequence, the longitudinal inequality of the yearly average
292 ($Sq_0(Y)$) might be influenced by the geomagnetic vertical component of the
293 non-dipole field.

294 The annual variation ($Sq_1(Y)$) also shows a close relation with the non-dipole
295 geomagnetic anomaly. $Sq_1(Y)$ is quite weak around the South Atlantic Ocean anomaly
296 and fairly strong around the Eurasia and Australia anomaly during both solar maxima
297 and minima years. Other than $Sq_0(Y)$, $Sq_1(Y)$ significantly correlate with *H* in both
298 hemispheres. The correlation coefficients between $Sq_1(Y)$ and *H* are 0.68/0.80 in the
299 northern/southern hemisphere during solar maximum, whereas only 0.11/0.13
300 between $Sq_1(Y)$ and *Z*.

301 In response to the annual change of the insolation and E-region ionization, the
302 local ionospheric conductivity enhances during local summer and weakens during
303 local winter. Hence, Yamazaki et al. [2009] inferred that the annual variation of the
304 ionospheric conductivity possibly resulted in the maximum ionospheric current
305 intensity during local summer and the minimum during local winter. In consideration
306 of the negative correlation between the geomagnetic field intensity and the
307 conductivity, the enhancement of *H* could attenuate the annual amplitude of the
308 conductivity and the ionospheric current intensity, leading to the decrease of $Sq_1(Y)$.

309 However, as shown in **Figures 7c** and **7d**, $Sq_I(Y)$ shows a positive correlation with *H*.
310 This is inconsistent with the conductivity mechanism stated above. In recent studies,
311 Takeda [2013a] proposed that the seasonal variation of Sq(Y) is affected by
312 inter-hemispheric field-aligned currents (IHFACs). These IHFACs are driven by the
313 imbalance of the Sq dynamo action, flowing from the summer to winter hemisphere
314 in the dawn sector and in the reverse direction in the noon sector [Yamashita and
315 Iyemori, 2002, Tomas et al., 2009, Park et al, 2011]. In the circumstance of the
316 IHFACs, Sq(Y) enhances in the summer hemisphere and diminishes in the opposite
317 hemisphere [Takeda, 2013a]. Because of high electric conductivity along the
318 magnetic field lines in the magnetosphere, the IHFAC is primarily determined by the
319 electric potential difference between the geomagnetic north-south conjugate-pair
320 points [Fukushima, 1979]. In other words, the annual change of inter-hemispheric
321 difference of the electric potential, which is produced by the interaction of the
322 geomagnetic horizontal field and neutral wind, plays an important role in the annual
323 variation ($Sq_I(Y)$).

324 It is widely accepted that the neutral wind blowing in summer is stronger than
325 that in winter, thus the asymmetry of the neutral wind in solstices could cause the
326 electric potential difference between the hemispheres. As the geomagnetic field at the
327 ionospheric footprints of a magnetic line becomes stronger, the electric potential
328 difference could be larger. This is in agreement with the positive correlation between
329 $Sq_I(Y)$ and *H*, suggesting that *H* might strongly influence the IHFACs. In fact, $Sq_I(Y)$
330 in the South American station PIL (7.8 nT) is very weak compared to the Australian

331 station KDU (9.6 nT) during solar active period, where *H* in PIL and KDU are
332 ~22000 nT and ~35000 nT respectively. $Sq_1(Y)$ in African stations, such as HER (6.0
333 nT), TSU (3.1 nT) and TAN (5.3 nT), are all fairly weak as well, where *H* also
334 remarkably diminishes due to SAO and AFR. Hence, the longitudinal difference of
335 $Sq_1(Y)$ might be primarily affected by the IHFACs and the geomagnetic horizontal
336 component.

337 The semiannual component $Sq_2(Y)$ shows distinct features with the above two
338 components. As shown in **Figure 8**, $Sq_2(Y)$ is very weak (about 2 nT) during solar
339 minima for most northern hemispheric stations, and becomes a little stronger during
340 solar maximum for some higher latitudinal stations. In contrast, $Sq_2(Y)$ in the
341 southern hemisphere significantly correlates with the geographic latitude regardless of
342 the solar activity, and $Sq_2(Y)$ in the higher latitude is obviously intense. These
343 features are consistent with the results using a magnetometer chain [Yamazaki et al,
344 2011]. Since the diurnal tide in the middle latitude atmosphere shows obvious peaks
345 at the equinoxes, identified by ground radar and satellite data, $Sq_2(Y)$ might be caused
346 by the semiannual variation of the tidal wind [Yamazaki et al., 2009; Pedatella, 2011].

347 In the southern hemisphere, $Sq_2(Y)$ shows an obviously negative correlation with
348 the horizontal component *H*. In particular, as *H* at four African stations (HER, HBK,
349 TSU and TAN) increases (~12000, ~13000, ~16000 and ~20000 nT) , $Sq_2(Y)$
350 decreases in turn (6.7, 6.4, 6.0 and 4.7 nT in solar maximum years). Considering the
351 negative correlation between *H* and the conductivity, the semiannual amplitude of
352 Sq(Y) might be affected by the ionospheric conductivity and *H*. On the other side,

353 $Sq_2(Y)$ is not related to the geomagnetic vertical component *Z*, implying that $Sq_2(Y)$
354 is independent on the convection electric field.

355 In summary, the seasonal variations of Sq(Y) at mid-low latitudes is investigated
356 in the present study. The annual variation ($Sq_1(Y)$) is very weak around South Atlantic
357 geomagnetic anomaly region and fairly strong around the Eurasia and Australia
358 anomaly during both solar maxima and minima years. $Sq_0(Y)$ and $Sq_1(Y)$ correlate
359 well with the geomagnetic component *Z* and *H* respectively. In addition, the
360 semiannual variation ($Sq_2(Y)$) in the southern hemisphere is prominent and shows a
361 strong dependence on the geographic latitude and the geomagnetic component *H*.

362 **Acknowledgements**

363 The authors acknowledge the World Data Center for Geomagnetism, Edinburgh
364 (http://www.wdc.bgs.ac.uk/catalog/master.html) and the observatories that provided
365 data used in the present study. The sunspot number data were obtained from
366 WDC-SILSO, Royal Observatory of Belgium, Brussels (http://sidc.be/silso/home/).
367 This work is supported by the Strategic Priority Research Program of Chinese
368 Academy of Sciences (Grant No. XDB41010304) and the National Natural Science
369 Foundation of China (41874080, 41674168, 41874197).

370 **References**

371 Banks, R. G. and E. C. Bullard (1966), The annual and 27 day magnetic variations,
372 Earth Planet. Sci. Lett., 1(3), 118-120
373 Bhargava, B. N. (1972), Semiannual and annual modulation of the magnetic field,
374 Planet. Space Sci., 20, 423-427
375 Briggs, B. H. (1984), The variability of ionospheric dynamo currents, J. Atmos. Sol.
376 Terr. Phys., 46, 419-429
377 Campbell, W. H. (1982), Annual and semiannual changes of the quiet daily variations
378 (Sq) in the geomagnetic field at North American locations, J. Geophys. Res.,

379 87(A2), 785-796, doi: 10.1029/JA087iA02P00785
380 Campbell, W. H. (1989), The regular geomagnetic-field variations during quiet solar
381 conditions, in Geomagnetism, 3, edited by J. Jacobs, chap. 6, pp.386-460,
382 Academic, San Diego, Calif.
383 Campbell, W. H. and S. Matsushita (1982), Sq currents: A comparison of quiet and
384 active year behavior, J. Geophys. Res., 87(A7), 5305-5308
385 Chapman, S., and J. Bartels (1940), Geomagnetism, Oxford Univ. Press, London.
386 Chapman, S., J. C. Gupta, and S. R. C. Malin (1971), The sunspot cycle influence on
387 solar and lunar daily geomagnetic variations, Proc. R. Soc. London Ser. A., 324,
388 1-15
389 Chen, G. X., et al. (2007) Statistical characteristics of the day-to-day variability in the
390 geomagnetic Sq field, J. Geophys. Res., 112, A06320,
391 doi:10.1029/2006JA012059
392 Currie, R. G. (1966), The geomagnetic spectrum-40 days to 5.5 years, J. Geophys.
393 Res., 71(19), 4579-4998
394 Forbes, J. M. And R. S. Lindzen (1976), Atmospheric solar tides and their
395 electrodynamic effect - I. The global Sq current system, J. Atmos. Terr. Phys., 38,
396 897-910
397 Fukushima, N. (1979), Electric potential difference between conjugate points in
398 middle latitudes caused in the ionosphere, J. Geomagn. Geoelectr., 31, 401-409
399 Hasegawa, M. (1960), On the position of the focus of the geomagnetic Sq current
400 system, J. Geophys. Res., 65, 1437-1447
401 Hibberd, F. H. (1985), The geomagnetic Sq variation - annual, semiannual and solar
402 cycle variations and ring current effects, J. Atmos. Terr. Phys., 47, 341-352
403 Le Sager, P. and T. S. Huang (2002), Longitudinal dependence of the daily
404 geomagnetic variation during quiet time, J. Geophys. Res., 107(A11), 1397, doi:
405 10.1029/2002JA009287
406 Matsushita, S. (1967), Solar quiet and lunar daily variation fields, in Physics of
407 Geomagnetic Phenomena, edited by S. Matsushita and W. Campbell, chap. II-1,
408 pp. 301-424, Academic, New York.
409 Matsushita, S. and H. Maeda (1965), On the geomagnetic solar quiet daily variation
410 field during IGY, J. Geophys. Res., 70(11), 2538-2558
411 Park, J., H. Luhr, and K. W. Min (2011), Climatology of the inter-hemispheric
412 field-aligned current system in the equatorial ionosphere as observed by CHAMP,
413 Ann. Geophys, 29, 573-582
414 Pedatella, N. M., J. M. Forbes and A. D. Richmond (2011), Seasonal and longitudinal
415 variations of the solar quiet (Sq) current system during solar minimum
416 determined by CHAMP satellite magnetic field observations, J. Geophys. Res.,
417 116, A04317, doi: 10.1029/2010JA016289
418 Rastogi, R. G. and K. N. Iyer (1976), Quiet day variation of geomagnetic H-field at
419 low latitudes, J. Geomagn. Geoelectr., 28, 461-479
420 Richmond, A. D. (1979), Ionospheric wind dynamo theory, J.Geomagn. Geoelec., 31,
421 287-310
422 Stening, R. J. (1971), Longitude and seasonal variations of the Sq current system,

Radio Sci., 6, 133-137
Stening, R. J. (1977), Field-aligned currents driven by the ionospheric dynamo, J. Atmos. Terr. Phys., 39(8), 933-937
Stening, R. J. (1995), Variations in the strength of the Sq current system, Ann. Geophys., 13, 627-632
Stening, R., T. Reztsovo and L. H. Minh (2005), Day-to-day changes in the latitudes of the foci of the Sq current system and their relation to equatorial electrojet strength, J. Geophys. Res., 110, A10308, doi: 10.1029/2005JA011219
Stening, R., T.Reztsova, and L. H. Minh (2007), Variation of Sq focus latitudes in the Australian/Pacific region during a quiet sun year, J. Atmos. Sol. Terr. Phys., 69, 734-740
Takeda, M. (1996), Effects of the strength of the geomagnetic main field strength on the dynamo action in the ionosphere, J. Geophys. Res., 101(A4), 7875-7880, doi: 10.1029/95JA03807
Takeda, M. (1999), Time variation of global geomagnetic Sq field in 1964 and 1980, J. Atmos. Terr. Phys., 61, 765-774
Takeda, M. (2002a), Features of global geomagnetic Sq field from 1980 to 1990, J. Geophys. Res., 107(A9), 1252, doi: 10.1029/2001JA009210
Takeda, M. (2002b), The correlation between the variation in ionospheric conductivity and that of the geomagnetic Sq field, J. Atmos. Terr. Phys., 64(15), 1617-1621
Takeda, M. (2013a), Difference in seasonal and long-term variations in geomagnetic Sq fields between geomagnetic Y and Z components, J. Geophys. Res., 118, 1-5, doi: 10.1002/jgra.50128
Takeda, M. (2013b), Contribution of wind, conductivity, and geomagnetic main field to the variation in the geomagnetic Sq field, J. Geophys. Res., 118, 4516-4522, doi: 10.1002/jgra.50386
Takeda, M., T. Iyemori and A. Saito (2003), Relationship between electric field and currents in the ionosphere and the geomagnetic Sq field, J. Geophys. Res., 108(A5), 1183, doi: 10.1029/2002JA009659
Takeda, M., Y. Yamada, and T. Araki (1986), Simulation of ionospheric currents and geomagnetic field variations of Sq for different solar activity, J. Atmos. Sol. Terr. Phys., 48, 277-287
Tarpley, J. D. (1973), seasonal movement of the Sq current foci and related effects in the equatorial electrojet, J. Atmos. Terr. Phys., 35, 1063-1071
Tomas, A. T., H. Luhr and M. Rother (2009), Mid-latitude solar eclipses and their influence on ionospheric current system, Ann. Geophys, 27, 4449-4461
Wagner, C. U. (1969), The 'semi-annual' variation of the solar daily quiet geomagnetic variation in the European region, Gerlands Beitr. Geophys., 78, 120-130
Wagner, C. U., D. Mohlmann, and K. Schafer (1980), Large-scale electric fields and currents and related geomagnetic variations in the quiet plasmasphere, Space Sci. Rev. , 26, 391-446
Xu, W. Y. and C. Y. Bai (2009), Role of the African magnetic anomaly in controlling the magnetic configuration and its secular variation, Chinese J. Geophys. (in

Chinese), 52(8), 1985-1992
Yamashita, S. and T. Iyemori (2002), Seasonal and local time dependences of the interhemispheric field-aligned currents deduced from the Orsted satellite and the ground geomagnetic observations, J. Geophys. Res., 107(A11), 1372, doi: 10.1029/2002JA009414
Yamazaki, Y. et al. (2009), Equivalent current systems for the annual and semiannual Sq variations observed along the 210°MM CPMN stations, J. Geophys. Res., 114, A12320, doi: 10.1029/2009JA014638
Yamazaki, Y., et al. (2011), An empirical model of the quiet daily geomagnetic field variation, J. Geophys. Res., 116, A1031, doi: 10.1029/2011JA016487
Yamazaki, Y., and A. Maute (2017), Sq and EEJ-A review on the daily variation of geomagnetic field caused by ionospheric dynamo currents, Space Sci Rev, 206, 299-405, doi: 10.1007/s11214-016-0282-z.

Figures Caption

Figure 1 Geographical distribution of the observatories used in this work. The background is the contour for the vertical component *Z* of the geomagnetic non-dipole field in 2000. Five large-scale anomalies are marked as SAO (the South Atlantic Ocean anomaly), AFR (Africa anomaly), ERA (Eurasia anomaly), AST (Australia anomaly), and NAM (North America anomaly).

Figure 2 Correlation of Sq(Y) at Kanoya (KNY) and sunspot number (SSN) in each month. One dot denotes the monthly mean value in the given month of one year from 1954 to 2010 at each subpanel. The linear regression line is plotted and the regression coefficient is shown at top right corner of each subpanel. The long-term variation of the annual SSN is shown in the bottom panel. Red and blue dots represent high and low solar activity, respectively.

Figure 3 Seasonal variation of Sq(Y) at typical stations in the Northern (a, c, e) and Southern (b, d, f) hemispheres. Months in the local summer are placed at the center for convenient comparison. Error bars represent the standard deviation. Red triangles and blue diamonds represent high and low solar activity years used in this study, respectively.

Figure 4 Annual and semiannual components of Sq(Y) for mid-latitude stations in northern and southern hemispheres. The solid and dotted lines represent the low and high solar activity, respectively.

Figure 5 Annual and semiannual components of Sq(Y) for typical stations in Asia-Australia and Europe-Africa sectors. The solid and dotted lines represent the low and high solar activity, respectively.

Fig.6 Correlation between $Sq_0(Y)$ and the geographic latitude, the geomagnetic horizontal component *H* and vertical component *Z* in the northern (a, c, e) and

511 southern (b, d ,f) hemispheres. Linear regression lines are drawn in each panel. Red
512 triangles and blue diamonds represent data in high and low solar activity, respectively.
513
514 **Figure 7** Same as in Figure 5, but for $Sq_1(Y)$.
515
516 **Figure 8** Same as in Figure 5, but for $Sq_2(Y)$.

Figures

Figure 1

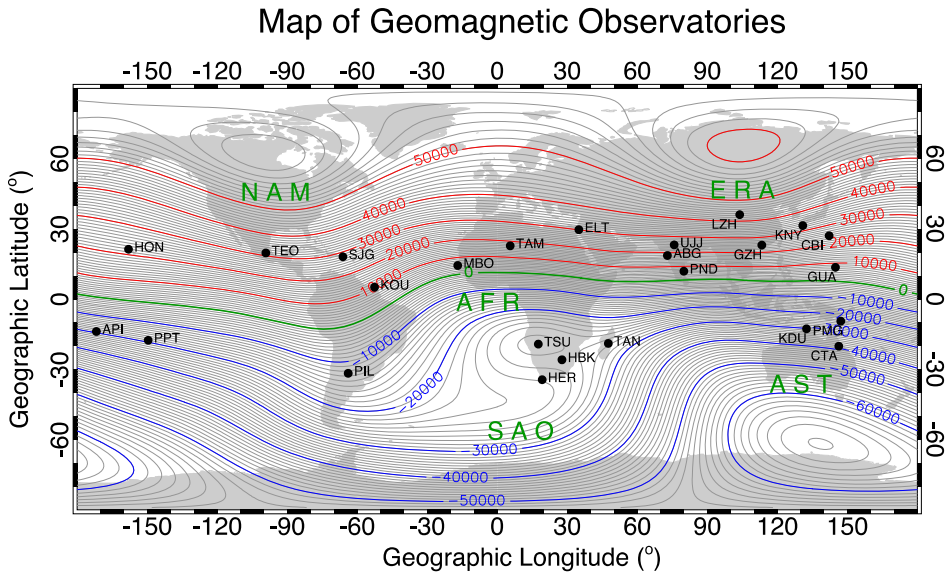

521 **Figure 2**

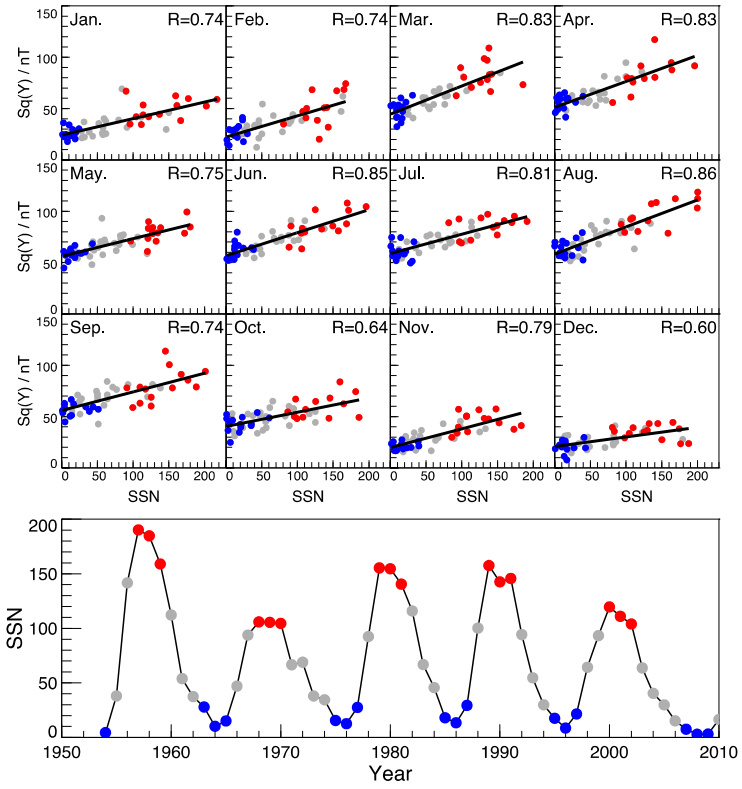

522

523

524 **Figure 3**

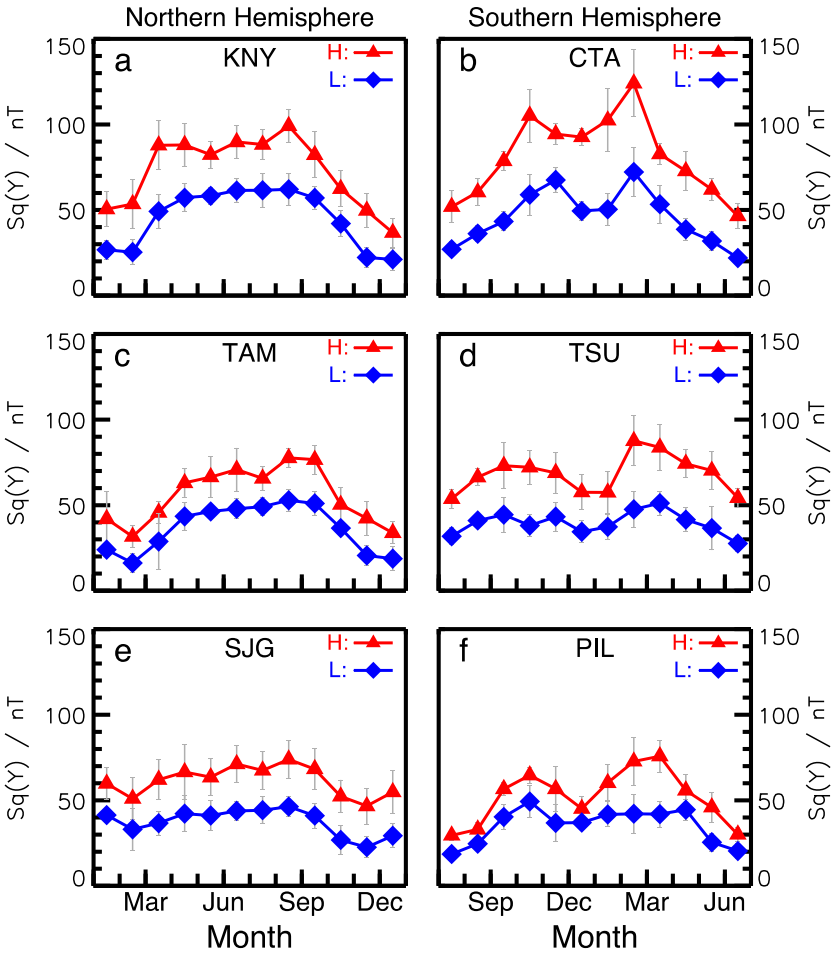

525

526

527 **Figure 4**

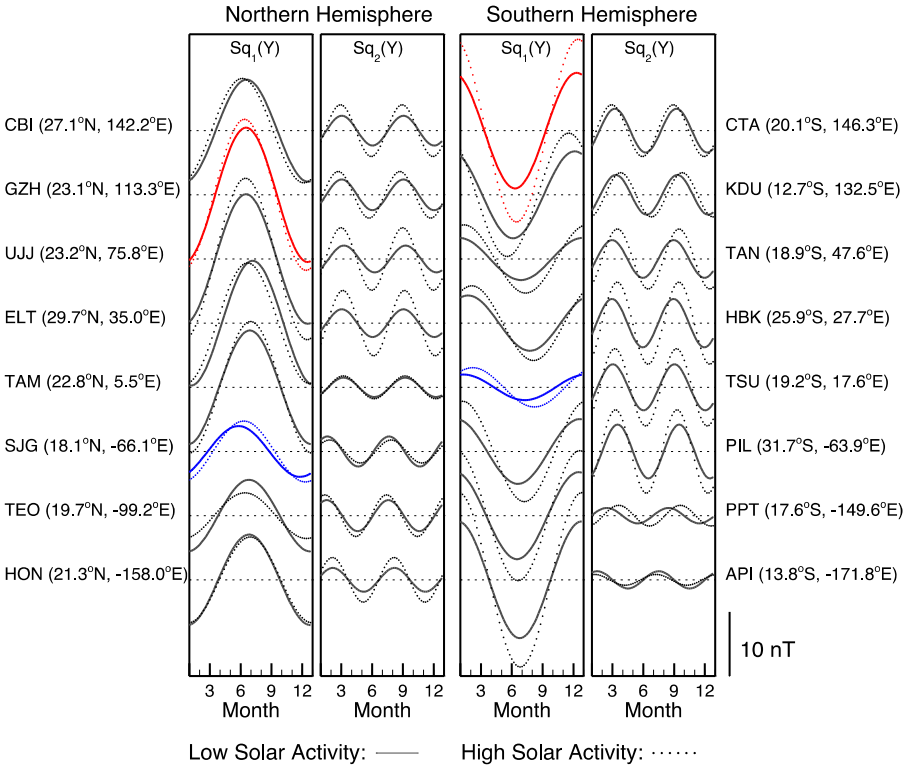

528

529

530

531 **Figure 5**

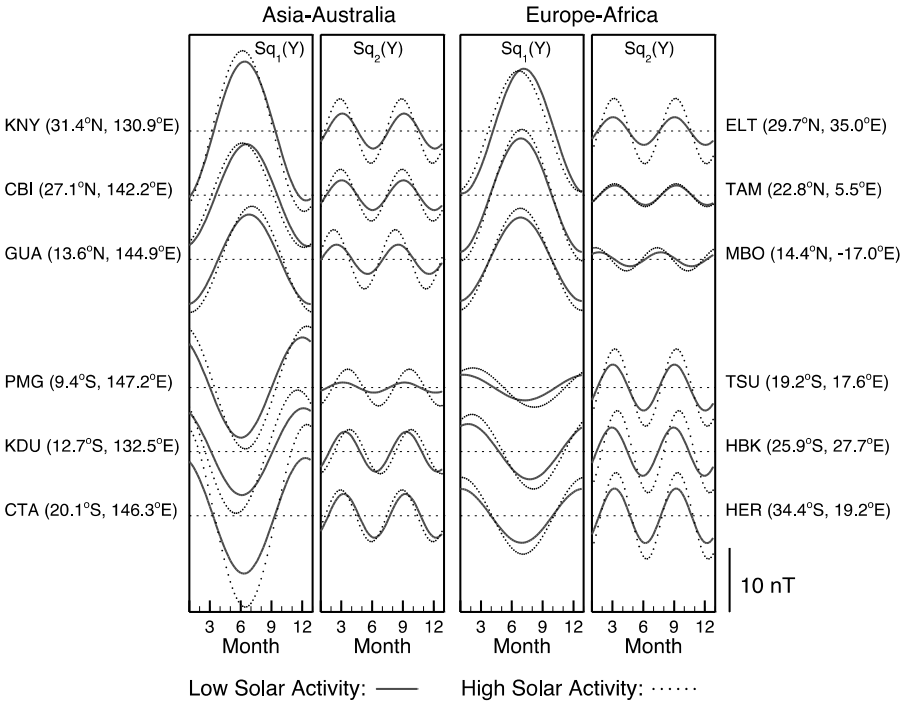

532

533

534

535 **Figure. 6**

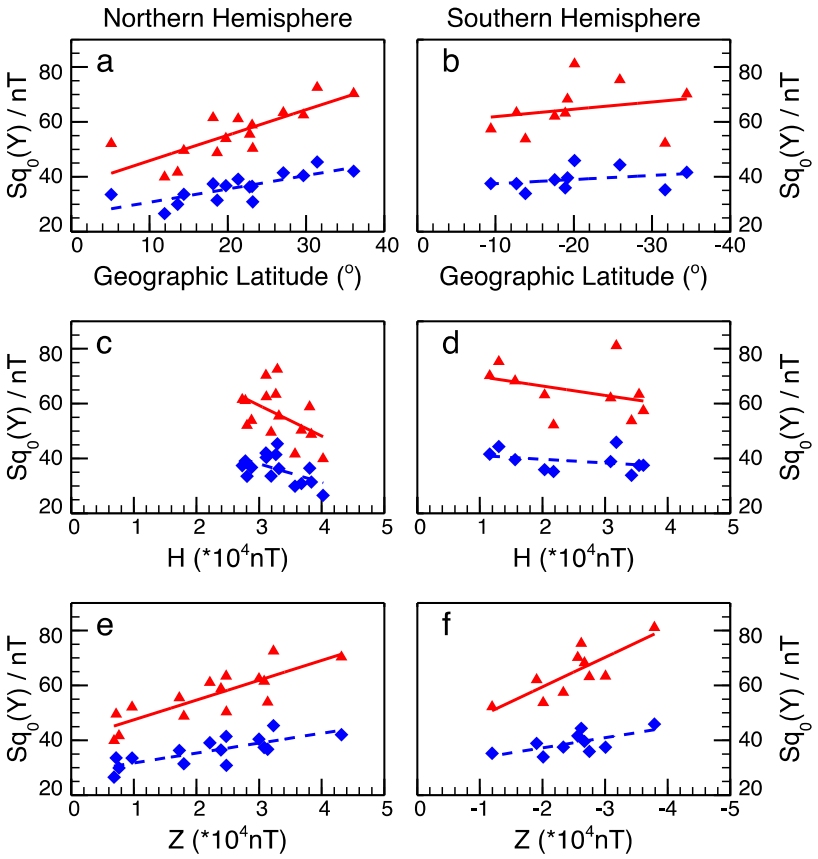

536

537

538 **Figure7**

539

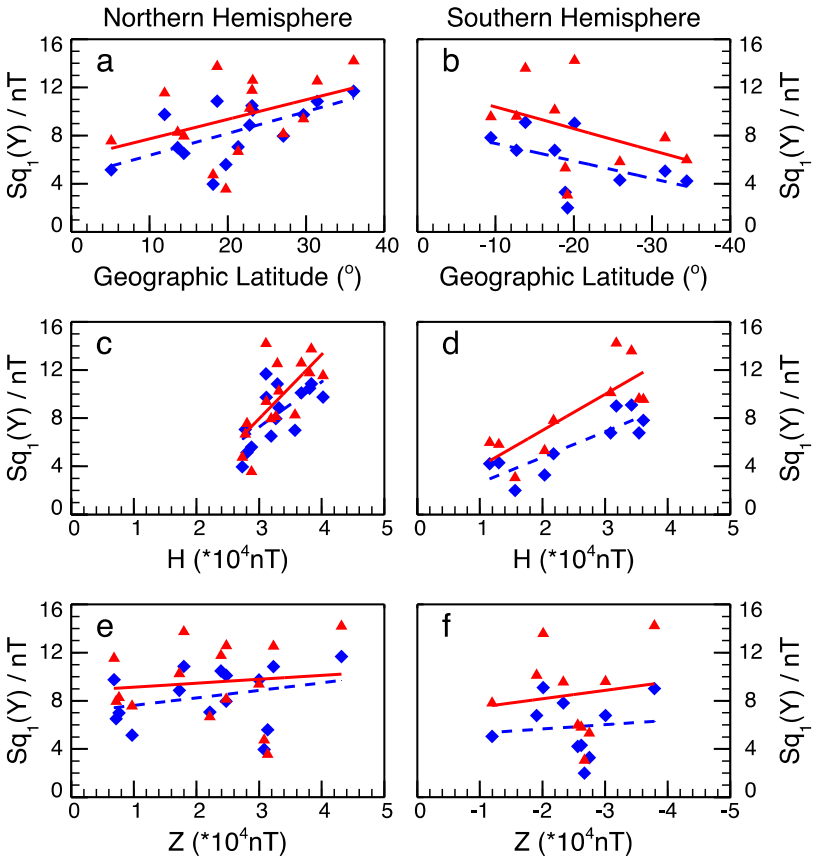

540

541

542 **Figure 8**

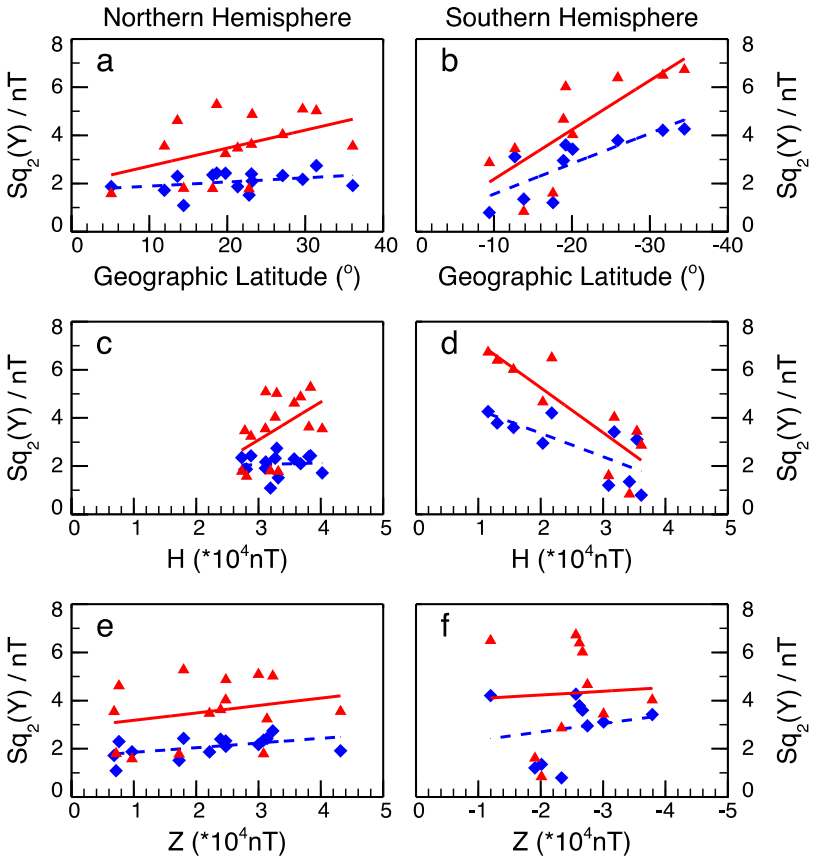

543

544

Table 1 List of the stations used in this study

Station	Code	GLat. (deg)	GLon. (deg)	GMLat. (deg)	GMLon. (deg)	Years
Hermanus	HER	-34.4	19.2	-33.9	83.7	57
Pilar	PIL	-31.7	-63.9	-21.4	7.0	22
Hartebeesthoek	HBK	-25.9	27.7	-27.1	94.1	39
Charters Towers	CTA	-20.1	146.3	-28.2	220.8	21
Tsumeb	TSU	-19.2	17.6	-18.7	85.6	43
Antananarivo	TAN	-18.9	47.6	-23.7	115.5	41
Pamatai	PPT	-17.6	-149.6	-15.1	285.0	43
Apia	API	-13.8	-171.8	-15.4	262.5	53
Kakadu	KDU	-12.7	132.5	-22.1	205.4	16
Port Moresby	PMG	-9.4	147.2	-17.4	220.3	34
Kourou	KOU	5.1	-52.6	14.9	19.6	15
Pondicherry	PND	11.9	79.9	2.8	152.1	15
Guam	GUA	13.6	144.9	5.2	215.4	54
MBour	MBO	14.4	-17.0	20.2	57.3	57
San Juan	SJG	18.1	-66.2	28.5	5.9	56
Alibag	ABG	18.6	72.9	10.1	146.0	57
Teoloyucan	TEO	19.8	-99.2	28.9	330.1	21
Honolulu	HON	21.3	-158.0	21.6	269.5	57
Tamanrasset	TAM	22.8	5.5	24.7	81.6	21
Guangzhou	GZH	23.1	113.3	12.7	184.6	41
Ujjain	UJJ	23.2	75.8	14.3	149.2	24
Chichijima	CBI	27.1	142.2	18.3	211.4	20
Eilat	ELT	29.7	35.0	26.3	111.8	13
Kanoya	KNY	31.4	130.9	21.8	200.5	53
Lanzhou	LZH	36.1	103.9	25.7	175.9	21

Note: Glat. and Glon. denote the geographic latitude and longitude. GMLat. and GMLon. denote the geomagnetic latitude and longitude. The column "Years" represents the time span of available data provided by each station.

Table 2 Correlation coefficients between Sq(Y) and the geographic latitude and components of the geomagnetic field

	Solar Activity	GLat.	H	Z	-GLat.	H	-Z
		Northern Hemisphere, n=15			Southern Hemisphere, n=10		
$Sq_0(Y)$	L	**0.76**	**-0.54**	**0.76**	0.31	-0.33	**0.65**
	H	**0.79**	-0.49	**0.83**	0.23	-0.36	**0.81**
$Sq_1(Y)$	L	**0.61**	**0.65**	0.28	-0.48	**0.85**	0.10
	H	0.41	**0.68**	0.11	-0.40	**0.80**	0.13
$Sq_2(Y)$	L	0.33	0.07	0.49	**0.79**	**-0.73**	0.19
	H	0.46	0.50	0.25	**0.78**	**-0.85**	0.05

Note: Glat. denotes the geographic latitude. *H* and *Z* denote the horizontal and vertical components of the geomagnetic field. Data satisfying the regression coefficient significance test ($R=0.514$, $p<0.05$ for the northern hemisphere and $R = 0.632$, $p < 0.05$ for the southern hemisphere) are marked in bold.